

First principle calculations of conductance within plane wave basis set via nonorthogonal Wannier-type atomic orbitals

Zhenyu Li and D. S. Kosov

Department of Chemistry and Biochemistry, University of Maryland, College Park, 20742, USA

We present a plane wave/pseudopotential implementation of the method to calculate electron transport properties of nanostructures. The conductance is calculated via the Landauer formula within formalism of Green's functions. Nonorthogonal Wannier-type atomic orbitals are obtained by the sequential unitary rotations of virtual and occupied Kohn-Sham orbitals, which is followed by two-step variational localization. We use these non-orthogonal Wannier type atomic orbitals to partition the Kohn-Sham Hamiltonian into electrode-contact-electrode submatrices. The electrode parts of the system are modeled by two metal clusters with additional Lorentzian broadening of discrete energy levels. We examined our implementation by modeling the transport properties of Na atomic wires. Our results indicate that with the appropriate level broadening the small cluster model for contacts reproduces odd-even oscillations of the conductance as a function of the nanowire length.

I. INTRODUCTION

The last decade has witnessed a remarkable miniaturization of conventional microelectronic devices. If this trend is to continue, elements of microelectronic circuits, e.g. transistors and contacts, will soon shrink to the size of a single molecule. One of the major goals in nanotechnology is the construction, measurement and modeling of electronic circuits in which molecular systems act as conducting elements¹. Accurate and reproducible measurements of current-voltage characteristics have been recently reported for atomic wires and single molecules^{2,3,4}. The experimental progress has been accompanied by considerable advances towards density functional theory based calculations of transport properties of nanostructures. This activity has been largely spurred on by development of several electronic structure codes for the first principle transport calculations.^{5,6,7,8}

The prerequisite for non-equilibrium Green's function calculation of conductance is the partitioning of the Kohn-Sham (KS) Hamiltonian into left/right electrodes and contact regions. Such partitioning is straightforward if one expands the KS wavefunctions as linear combinations of atomic orbitals^{5,6,7,8} but it becomes a formidable theoretical problem if the plane waves are used for a representation of the KS orbitals. One of the aims of this paper is development of a theoretical scheme to the partition of the KS Hamiltonian within plane wave basis set.

It has been recently proposed that Wannier functions can be used to link plane wave electronic structure and Green's function transport calculations.^{9,10} Wannier functions are localized in coordinate space and are obtained by an unitary transformation of the KS orbitals. The number of Wannier functions is typically much smaller than the dimension of Gaussian-type basis sets. The additional advantage is that, we treat the electrode and the wire at the same level of theory within the Wannier functions basis whereas it is not possible if one uses Gaussian basis set. The quality of Gaussian-type atomic basis set can not be easily controlled, which

makes the results of calculation sensitive to a particular choice of basis functions. In principle, these problems do not exist for plane wave basis set, where its quality is simply controlled by a single parameter, the cutoff energy.¹¹ By increasing the cutoff energy, we can always get converged results. There are two disadvantages which makes standard Wannier functions inapplicable for the calculations of transport properties. First, Wannier functions are defined for occupied KS orbitals and if the same localization scheme is directly used for the virtual orbitals it typically leaves them as delocalized as they were before the unitary transformation. Second, the centers of these localized Wannier functions are not controllable before minimization. To address both issues, we have developed the localization technique which yields non-orthogonal Wannier-type atomic orbitals (NOWAOs) from the plane-wave based KS orbitals. NOWAOs are the maximally localized functions defined via the set of unitary transformations of occupied and virtual KS orbitals. Our scheme is based upon the combination of two localization techniques: Thygesen-Hansen-Jacobsen partially occupied Wannier functions¹² and Mortensen-Parrinello non-orthogonal localization.¹³ Combined together, these two techniques are used to include the virtual KS orbitals and to shift the Wannier centers from bonds to atoms.

One additional ingredient, which is necessary for calculations of conductance, is the Green's function of the electrodes. In this paper, we represent the leads by two small clusters with additional Lorentzian broadening of the energy levels.

We have implemented the working equations within a plane-wave/pseudopotential code¹⁴ and we will demonstrate the numerical accuracy of implementation for some prototypical test examples. The remainder of the paper is organized as follows. In Section II, we describe the details of our method to calculate the conductance of nanostructures, and its application to sodium atomic wires is given in Section III. In Section IV, we conclude the paper.

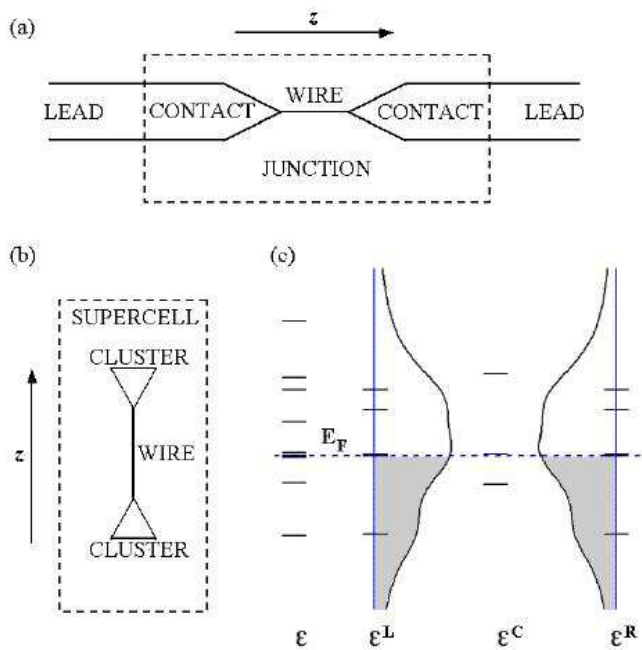


FIG. 1: (a) Schematic representation of an atomic/molecular scale junction system for electronic transportation. (b) Simplified transportation model used in our method. (c) Energy levels for junction system containing three-atom sodium wire. Density of states obtained by Lorentzian broadening of the electrode levels are also shown. See text for details.

II. METHOD

A. Partitioning of the Hamiltonian

We begin with the Kohn-Sham equation for the entire nanowire junction

$$H|\psi_i\rangle = E_i|\psi_i\rangle, \quad (1)$$

where H is the Kohn-Sham Hamiltonian and $|\psi_i\rangle$ is the Kohn-Sham orbital. The next step is the partitioning of the system into three parts: two electrodes and wire (typically atomic or molecular wire plus parts of the lead) as it is shown in Fig. 1. The partitioning of the system results into the partitioning of the Hamiltonian to seven sub-matrices (left lead, contact, right lead and the lead-wire interactions) and it is performed by transforming the representation of the KS Hamiltonian from KS orbitals to atomically localized basis sets:

$$|\psi_i\rangle = \sum_{n=1} U_{in}|w_n\rangle, \quad (2)$$

where U_{in} is a unitary transformation and $|w_n\rangle$ form atomically localized complete basis set. The unitary transformation U_{in} is applied to the KS Hamiltonian

$$H = \sum_i |\psi_i\rangle E_i \langle \psi_i| = \sum_{nm} |w_n\rangle H_{nm} \langle w_m| \quad (3)$$

with

$$H_{nm} = \sum_i U_{ni}^* E_i U_{im} \quad (4)$$

and yields the partitioning of the Hamiltonian into electrode-wire-electrode sub-matrices:

$$\mathbf{H} = \begin{pmatrix} \mathbf{H}_L & \mathbf{H}_{WL}^\dagger & 0 \\ \mathbf{H}_{WL} & \mathbf{H}_W & \mathbf{H}_{WR} \\ 0 & \mathbf{H}_{WR}^\dagger & \mathbf{H}_R \end{pmatrix}. \quad (5)$$

If the basis set $|\omega_n\rangle$ is not orthogonal, the analogous partitioning should be performed for the overlap matrix \mathbf{S} ($S_{mn} = \langle \omega_m | \omega_n \rangle$). Matrices \mathbf{H} and \mathbf{S} can be defined if indexes n and m in H_{nm} (3) are associated with the atomic positions. But this is not the case when periodic boundary conditions are employed and the KS orbitals are expanded in plane waves:

$$\psi_i(\vec{r}) = \frac{1}{\sqrt{\Omega_{cell}}} \sum_{\vec{G}} C_{i\vec{G}} \exp(i\vec{G}\vec{r}), \quad (6)$$

where $C_{i\vec{G}}$ are the expansion coefficients. The plane waves $\exp(i\vec{G}\vec{r})$ do not have any reference to the atomic positions and therefore the partitioning of the KS Hamiltonian into electrode-wire-electrode subspaces can not be performed directly within the plane wave representation. Several groups have attempted to overcome this difficulty by Wannier function representations of the KS orbitals.^{9,10}

B. Non-orthogonal Wannier-type Atomic Orbitals

Wannier functions are localized functions which span the same space as the eigenstates of a band or a group of bands. Traditional Wannier functions are obtained by transforming Bloch representation to real space representation,¹⁵ in which Bloch vector \vec{k} is substituted by the lattice vector \vec{R} of the unit cell where the orbital is localized.

$$\begin{aligned} |\vec{R}n\rangle &= \frac{\Omega_{cell}}{(2\pi)^3} \int_{BZ} |\psi_{n\vec{k}}\rangle e^{i\phi_n(\vec{k}) - i\vec{k}\cdot\vec{R}} d\vec{k} \\ &= \frac{\Omega_{cell}}{(2\pi)^3} \int_{BZ} \sum_m U_{mn}^{(\vec{k})} |\psi_{m\vec{k}}\rangle e^{-i\vec{k}\cdot\vec{R}} d\vec{k} \end{aligned} \quad (7)$$

where $U_{mn}^{(\vec{k})}$ is an arbitrary unitary matrix. The integration in eq.(7) is done in reciprocal space within the whole Brillouin zone. The vector \vec{k} equals zero for disordered systems like nanostructures or molecular wire junctions. In this case, the Wannier functions is defined via the unitary transformation of the KS orbitals¹⁶

$$|\omega_n\rangle = \sum_m U_{mn} |\psi_m\rangle. \quad (8)$$

There are several different schemes to define unitary matrix U_{mn} and the choice the unitary transformation can

be tailored to particular applications. Finding the maximally localized Wannier functions is pivotal for the partitioning of the Hamiltonian. Although there are several possible ways to define maximally localized Wannier functions, the method of minimization of the mean square spread stands out.^{17,18}

Wannier functions are traditionally constructed only from the occupied KS orbitals. Occupied Wannier functions are located on the chemical bonds, which sometimes makes the partition of junction systems difficult. The additional complication is that the sum in eq.(3) runs over all KS orbitals (occupied and virtual) and due to the completeness requirement it is necessary to include as many virtual KS orbitals in the consideration as possible. Therefore, to be used in transport calculations Wannier functions should be constructed in such a way that (a) they are atomically localized and (b) they include both occupied and virtual KS orbitals. The above two requirements are interconnected since to get atomic centered Wannier functions, we must anyway combine unoccupied anti-bonding states with occupied bonding states. The extraction of anti-bonding states from the entire set of virtual orbitals is difficult computational problem, since unoccupied anti-bonding states are mixed with some scattering states originating from periodic boundary conditions.

Following Thygensen, Hansen and Jacobsen¹² we begin the localization of the KS eigenstates by constructing the linear combination of the virtual orbitals

$$|\phi_l\rangle = \sum_{m=1}^{N-M} c_{ml} |\psi_{M+m}\rangle, \quad (9)$$

where N is the number of KS orbitals and M is the number of occupied states. Partially occupied Wannier functions are written as¹²

$$|\tilde{\phi}_n\rangle = \sum_{m=1}^M U_{mn} |\psi_m\rangle + \sum_{l=1}^L U_{M+l,n} |\phi_l\rangle, \quad (10)$$

with L being the number of unoccupied anti-bonding states. The optimal value of L is yet to be determined.

We minimize the following localization functional

$$\Omega = \sum_n [\langle \tilde{\phi}_n | r^2 | \tilde{\phi}_n \rangle - \langle \tilde{\phi}_n | \tilde{r} | \tilde{\phi}_n \rangle^2] \quad (11)$$

to choose a suitable unitary transformation U_{mn} and to obtain the maximally-localized Wannier functions.^{17,18} Minimization of functional Ω is equivalent to maximization of the functional

$$\Xi = \sum_n \sum_I w_I |Z_{nn}^I|^2, \quad (12)$$

where matrix \mathbf{Z}^I is defined as

$$Z_{mn}^I = \langle \tilde{\phi}_m | e^{-i\vec{G}_I \cdot \vec{r}} | \tilde{\phi}_n \rangle, \quad (13)$$

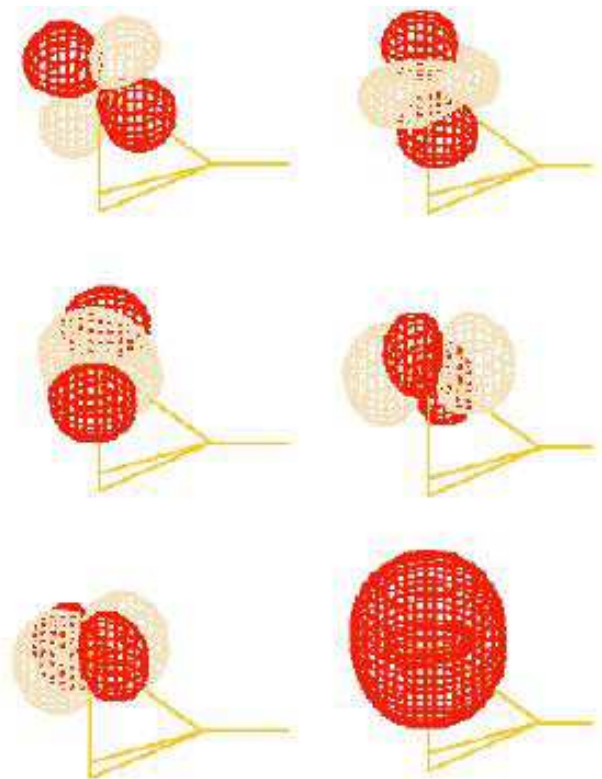


FIG. 2: (Color online) Non-orthogonal Wannier-type atomic basis functions (NOWAOs) for one gold atom in a simple gold junction system. Only half of the junction is shown.

with \vec{G}_I and w_I being the reciprocal lattice vectors and corresponding weights.¹⁶ For simple orthorhombic supercell, I ranges from 1 to 3, corresponding to x , y , and z . In practical implementation, \mathbf{Z}^I is calculated by $\mathbf{Z}^I = \mathbf{U}^\dagger \mathbf{Z}_0^I \mathbf{U}$, with \mathbf{Z}_0^I defined as

$$(Z_0^I)_{mn} = \langle \psi_m | e^{-i\vec{G}_I \cdot \vec{r}} | \psi_n \rangle. \quad (14)$$

Analytical gradients of functional Ξ (12) are necessary to perform effective maximization. If we write the unitary matrix at iteration i as $\mathbf{U}_i = \mathbf{U}_{i-1} \exp(-\mathbf{A})$, then the gradients of functional Ξ with respect to \mathbf{A} can be approximated as

$$(d\Xi/dA)_{ij} = \sum_I w_I [Z_{ji} (Z_{jj}^* - Z_{ii}^*) - Z_{ij}^* (Z_{ii} - Z_{jj})]. \quad (15)$$

The gradient with respect to the coefficient matrix c_{lm} is computed by the following formula¹²

$$(d\Xi/dc^*)_{ij} = \sum_I w_I [[\mathbf{Z}_0 \tilde{\mathbf{U}} \text{diag}(\mathbf{Z}^\dagger) + \mathbf{Z}_0^\dagger \tilde{\mathbf{U}} \text{diag}(\mathbf{Z})] \mathbf{U}^\dagger]_{N+i, N+j}, \quad (16)$$

where $\text{diag}(\mathbf{Z})$ is the diagonal part of matrix \mathbf{Z} , and $\tilde{\mathbf{U}}$ is the rotation matrix from KS orbitals to partly occupied

Wannier functions with dimension $N \times (M + L)$. The orthonormality constraint on matrix \mathbf{c} is invoked through a set of Lagrange multipliers. The steepest descent method is used to maximize Ξ . After the maximization, the unoccupied anti-bonding states are obtained from the coefficient matrix \mathbf{c} through Eq.(9).

A final set NOWAOs is computed via the additional rotation of partially occupied Wannier functions (10):

$$|\omega_n\rangle = \sum_{m=1}^{M+L} V_{mn} |\tilde{\phi}_m\rangle. \quad (17)$$

Rotation matrix V_{nm} is defined by minimizing the following function¹³ independently for each n :

$$\Omega_n = \langle \omega_n | p(\vec{r} - \vec{R}_n) | \omega_n \rangle \quad (18)$$

The weight function $p(\vec{r})$ is chosen in such a way that it has a minimum at $r = 0$ to localize each $|\omega_n\rangle$ around \vec{R}_n . Following Mortensen and Parrinello¹³ we select function $p(\vec{r})$ as

$$p(\vec{r}) = \sum_{\alpha=x,y,z} \left[1 - \cos\left(\frac{2\pi}{L} r_\alpha\right) \right]. \quad (19)$$

Ω_n can also be written in the matrix form:

$$\Omega_n = (\mathbf{V}^\dagger \mathbf{P}^{(n)} \mathbf{V})_{nn} = \vec{v}_n^\dagger \mathbf{P}^{(n)} \vec{v}_n, \quad (20)$$

where \vec{v}_n is the n th column of \mathbf{V} , and

$$P_{ij}^{(n)} = \langle \tilde{\phi}_i | p(\vec{r} - \vec{R}_n) | \tilde{\phi}_j \rangle \quad (21)$$

with $|\tilde{\phi}\rangle$ being the set of partially occupied Wannier functions obtained by maximization of Ξ . Matrix element $\mathbf{P}^{(n)}$ are calculated only once and stored for every n . The minimum of Ω_n is obtained when \vec{v}_n is equal to the normalized eigenvector corresponding to the smallest eigenvalue of $\mathbf{P}^{(n)}$. If we need several NOWAOs for a single atomic site, the corresponding number of smallest eigenvectors should be chosen. The number of anti-bonding states necessary for the localization (L in eq.(10) can now be computed by the following formula:

$$L = N_A N_{LE} - M, \quad (22)$$

where N_A is the number of atoms in the system and N_{LE} is the number of the lowest eigenstates included into Mortensen-Parrinello localization. For example, for gold atom, which is typical electrode material in molecular electronics, five d -type and one s -type NOWAOs per atom are need. In Fig. 2, we plot the generated six NOWAOs for a gold atom in a simple gold wire junction system. We can clearly see that these six NOWAOs reflect the s and d characters of gold atom.

C. Conductance Formula

The starting point for the conductance calculations is the Landauer formula¹⁹

$$G = \frac{2e^2}{h} T(E_F), \quad (23)$$

where T is the transmission function and E_F is the Fermi energy of the electrodes. Having obtained the partitioned Hamiltonian (5), we can compute transmission as the trace of Green's function \mathbf{G} and coupling matrices $\mathbf{\Gamma}_{L/R}$:⁷

$$T(E) = \text{Tr}[\mathbf{\Gamma}_L(E) \mathbf{G}(E) \mathbf{\Gamma}_R(E) \mathbf{G}^\dagger(E)]. \quad (24)$$

The matrices \mathbf{G} and $\mathbf{\Gamma}_{L/R}$ are expressed by the matrix blocks of the Hamiltonian \mathbf{H} , overlap \mathbf{S} , self energy $\mathbf{\Sigma}$:

$$\mathbf{G}(E) = [E\mathbf{S}_W - \mathbf{H}_W - \mathbf{\Sigma}_L - \mathbf{\Sigma}_R]^{-1} \quad (25)$$

and

$$\mathbf{\Gamma}_{L/R}(E) = i[\mathbf{\Sigma}_{L/R} - \mathbf{\Sigma}_{L/R}^\dagger]. \quad (26)$$

The self-energies $\mathbf{\Sigma}_{L/R}$ are defined via the Green's function of the left and right electrodes \mathbf{g} and the electrode-wire interactions:

$$\mathbf{\Sigma}_{L/R}(E) = (E\mathbf{S}_{WL/R} - \mathbf{H}_{WL/R}) \mathbf{g}_{L/R}(E) (E\mathbf{S}_{WL/R}^\dagger - \mathbf{H}_{WL/R}^\dagger). \quad (27)$$

It is not possible to include the entire leads in the practical calculations. The interaction between the wire and the infinitely large leads is accounted by the self-energy. Different theoretical models have been proposed to obtain \mathbf{g} . The most accurate schemes rely on the surface Green's function method. Even with some special techniques, such as transfer matrix^{20,21} and decimation technique²², the computation of surface Green's function is complex and time-consuming. Since detailed experimental geometrical structures of leads and a nanowire are unclear in most cases, it enables us to use the simpler models for the leads. In this paper, the electrode is represented by a metal cluster with additional energy level broadening²³. This model has proven to be very successful in estimation of the bulk density of states from small cluster calculations.^{24,25} As shown in APPENDIX A, the Lorentzian broadening σ in the electrode density of state is the same as is positive infinitesimal σ in the electrode Green's function:

$$\mathbf{g} = [(E + i\sigma)\mathbf{S}_{L/R} - \mathbf{H}_{L/R}]^{-1}. \quad (28)$$

III. TEST RESULTS

A. Computational methods

To illustrate the performance of our method we computed transport properties of Na nanowire. Nanowires of

metal atoms have recently attracted much attention because of their fundamental and technological importance. In particular, sodium atomic wire has been studied both experimentally^{26,27,28} and theoretically.^{29,30,31,32,33} It was found that the conductance of Na wires exhibits even-odd oscillation as a function of the number of atoms in the wire. The conductance for odd sodium atom numbered wire is close to the quantum of conductance G_0 ($2e^2/h$), while the conductance for even sodium atom numbered wires is smaller than G_0 . Different implementation and junction models lead to different the values of the conductance for even numbered nanowires ($0.5 - 0.9 G_0$).^{29,30,31,32,33} We use Na atomic nanowire as a proving ground for our implementation and we aim to reproduce the odd-even oscillation and values of the conductance.

The calculations were performed using our implementation of the formalism presented here in the CPMD package¹⁴. All systems were treated employing periodic boundary conditions and the KS orbitals were expanded in plane waves (50 Ry cutoff) at the Γ point of the Brillouin zone. We used local density approximation for the exchange and correlation functional and Stumpf, Gonze, and Schettler pseudopotentials³⁴ for core electrons. The system is simulated by a cluster in a large supercell. The size of supercell is chosen in such a way that the distance between the nearest atoms in the neighboring cells is larger than 8.5\AA , so that the interaction between supercell images is negligible. An extensive set of the KS virtual orbitals is computed via Lanczos diagonalization³⁵ to ensure that all possible unoccupied anti-bonding states are included. To speed up convergence of the self-consistent iterations, free energy functional³⁶ is used with the electronic temperature $T = 300$ K. Since sodium is a single valent atom, only one NOWAO per Na atom is constructed from the KS orbitals.

The whole system is divided into three parts: left electrode, central wire, and right electrode. The electrode part is obtained by cutting a few atoms from Na (001) surface. In particular, as shown in the inset of Fig. 3, we cut a five-atom cluster, which is composed of square four-atom base and apex atom. The geometry of this five-atom cluster is fixed to the bulk values. The wire part is a single chain of Na atoms, where the distance between the atoms is constrained to the nearest neighbor distance in the bulk system. The distance between the electrode part and the wire part is optimized. The optimized value d is listed in Table I and it shows small $\sim 0.1 - 0.2 \text{\AA}$ odd-even oscillation as the length of the wire varies. We use optimized value of electrode-wire separation in all our calculations.

Let us take a three-atom Na wire as an example to illustrate conductance calculations by the method we described in the previous section.

First, electronic structure of the whole system is calculated, and a set of KS orbitals is obtained. The number of KS orbitals should be large enough to include all unoccupied anti-bonding states. Fig.3 shows the conductance

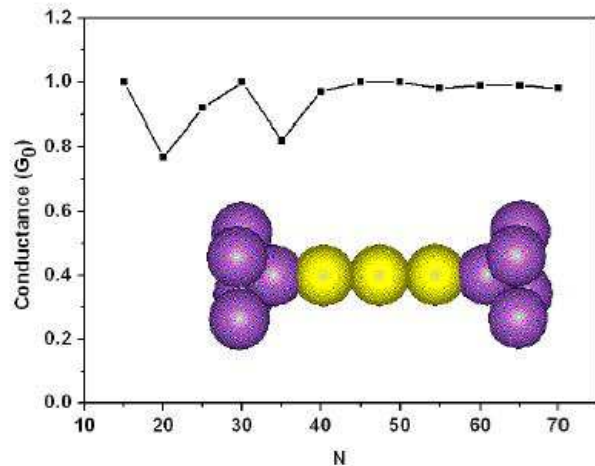


FIG. 3: Conductance of three-atom Na atomic wire as a function of number of Kohn-Sham orbitals calculated to construct the NOWAOs. The inset shows the geometry of this junction system.

as a function of the number of KS orbitals included in the localization procedure to define NOWAOs. The deviation of the conductance from the correct value ($1 G_0$) vanishes rapidly as the number of virtual KS orbitals is increased. Our test calculations illustrate the number of the virtual KS orbitals can be adjusted to achieve any desired level of accuracy in the conductance calculations. The results on Fig.3 demonstrate that 45 virtual KS orbitals are sufficient to get the converged result for three atom Na wire.

Second, this set of KS orbitals is used to construct NOWAOs, with which Hamiltonian matrix \mathbf{H} and overlap matrix \mathbf{S} are calculated. By solving the corresponding generalized eigenvalue problem, we get a set of energy levels ϵ for the whole junction system, as shown in the left column of Fig. 1c. The differences between these eigenlevels and the Kohn-Sham energies are very small, especially for occupied state. At the same time, partition of \mathbf{H} and \mathbf{S} is implemented, and the energy levels of electrodes, ϵ^L and ϵ^R , are obtained by solving the generalized eigenvalue problem for the corresponding submatrices.

Third, we introduce Lorentzian broadening of the left and right energy levels to continuous density of states, to compute the self-energy matrices. The broadening parameter σ is chosen to be 0.025 Hartree here, and the effect of broadening parameter on conductance will be discussed later. The transmission probability is computed by using section II.B equations. The peak positions of the transmission curve can be considered as renormalized eigenlevels of the central three-atom Na wire coupled to the electrodes (ϵ^C in Fig. 1).

In units of G_0 , the conductance equals to the value of the transmission at Fermi energy of the leads. Fermi energy for the electrode is not known *a priori* and it has to be computed within the approach. There are two

schemes to compute Fermi energy of the electrodes. The first one determines the Fermi energy at which the integrated density of states should be equal to the number of electrons in the electrode cluster.²³ The charge population of the electrode cluster is calculated by $\rho_{L/R} = \sum_{i \in L/R} (\mathbf{S}^{1/2} \mathbf{P} \mathbf{S}^{1/2})_{ii}$, where \mathbf{P} is the density matrix on NOWAOs basis set, which is obtained from the generalized eigenvalue problem of the whole junction cluster system. The other one is more simple, we can just use the Fermi energy of the whole junction system. When the electrode clusters are very large, both methods become equivalent. For the five-atom model used here, we find the later method is preferable and it yields 1 G_0 value of the conductance of the three-atom Na wire system.

B. Oscillation of Conductance

The most important feature of electronic current flow through Na atomic wires is that the conductance oscillates as a function of the number of atoms in the wire. We calculate the conductance of Na atomic wires with length range from 2 to 5 atoms. The odd-even oscillation of the conductance is well reproduced as shown in Fig. 4a. The conductance for $N = 3$ and $N = 5$ is one unit conductance G_0 , while the conductance for $N = 2$ and $N = 4$ is about 0.7 G_0 . The transmission curves for these wire systems are plotted in Fig. 4b. We can see that the number of sharp peaks in the transmission curves, i.e. the number of resonant states, is equal to the number of atoms in the wire. The low temperature transport properties are mainly determined by the states near the Fermi energy. There is a resonant state at the Fermi energy for odd numbered Na wires, but there is no such state for even numbered Na wires. This is exactly the reason of the even-odd oscillation behavior of the conductance.^{30,32}

C. Eigenchannels

Since there are multiple peaks in the transmission curve, it is interesting to see if sodium wires are single channel conductor as we expected for monovalent atomic chain. By defining

$$\mathbf{t} = \mathbf{\Gamma}_L^{\frac{1}{2}} \mathbf{G}^R \mathbf{\Gamma}_R^{\frac{1}{2}} \quad (29)$$

the transmission can be written as $T(E) = \text{Tr}(\mathbf{t} \mathbf{t}^\dagger)$. We can decompose the transmission to the combination of some eigenchannels diagonalizing the matrix $\mathbf{t} \mathbf{t}^\dagger$.³⁷ For sodium wires, we get only one non-zero eigenvalues at any energy, which is the manifestation of a single channel conduction mechanism.

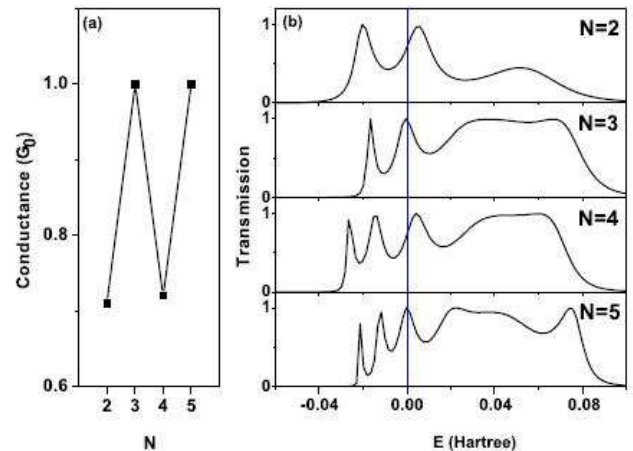


FIG. 4: (a) Conductance oscillation of sodium atomic wire with its length. (b) Transmission curves of the sodium atomic wires. Fermi energy is set to zero.

TABLE I: Distance between electrode and wire d (in Å), and conductance of the Na atomic wire junction systems. The length of Na wire N ranges from 2 to 5 atoms. The electrode part of the junction system is modeled by one (E1 model) or five (E5 model) Na atoms. Conductance for four different broadening parameter 0.02, 0.025, 0.03, and 0.04 Hartree are listed. See text for more details.

N	d	E1 Model				E5 Model				
		0.02	0.025	0.03	0.04	d	0.02	0.025	0.03	0.04
2	3.004	0.33	0.43	0.50	0.57	3.078	0.64	0.71	0.75	0.77
3	3.070	0.99	0.99	0.98	0.97	3.270	0.99	1.00	1.00	0.99
4	3.024	0.65	0.81	0.92	1.00	3.097	0.71	0.72	0.72	0.69
5	3.042	0.99	0.99	0.99	0.99	3.221	1.00	1.00	0.98	0.96

D. Electrode Cluster Model

In our method, the electrode is approximated by a small cluster with proper level broadening. Therefore it is important to understand how the results of our calculations are affected by the cluster size and by the choice of the broadening.

The size of the electrode cluster should be big enough, so that charge neutrality is maintained for the junction system. As it was discussed in the sections III.A and III.B the five-atom electrode model is sufficient to simulate the transport behavior of sodium wires in our method.³⁸ It is already a very small size comparing to typically used models for electrodes, but it is interesting to see if a smaller cluster still works in our method. For this purpose, we also check the simplest one-atom model. The results are listed in Table I. Comparing to the five-atom model, the oscillation strength of the optimized distance between electrode and wire is smaller. We can see that the conductance for one-atom model still exhibits the even-odd oscillation, but the conductance of

even numbered wires are not very stable anymore. This result indicates that the one-atom electrode model provides the oversimplified description of the system.

It is also important to test if the broadening parameter strongly effects results of the transport calculations. We analyzed the conductances for all wires by varying the broadening parameter σ from 0.02 to 0.04 Hatree, and list the result in Table I. We find that for large electrode model, the conductance is not very sensitive to the variations of σ , especially for odd-numbered wire system. For one-atom electrode model, the conductance changes significantly as σ varies. This is because there is only one electrode energy level for one-atom model, and the shape of the density of states at E_F strongly depends on the broadening parameter.

There is another conductance calculation method for single channel nanowire.^{30,39} It is based on Friedel sum rule and also relies on the eigenlevel broadening technique to represent continuum of states in the contact. In that method, the eigenvalues of the whole junction system ϵ are broadened to obtain density of states, thus the broadening parameter should be smaller than the resonance spacing but larger than single particle level spacing for electrode. To satisfy this constraint, the spacing of ϵ^L and ϵ_R should be much smaller than that of ϵ^C , and therefore much larger electrode clusters should be used in Friedel sum rule based calculations. In our method, however, if the broadening parameter is comparable to the resonance spacing, we still get very accurate results. Therefore, much smaller metal clusters can be used to model electrodes within our implementation.

IV. CONCLUSIONS

We have developed and implemented a plane wave based method to calculate the conductance of nanostructures. The fundamental quantity in the present implementation is NOWAOs which are obtained by the multi-step localization of KS orbitals. NOWAOs are used to partition KS Hamiltonian to electrode-wire-electrode submatrices that is necessary step for the Green's function based conductance calculations. The electrode parts are modeled by small clusters with proper broadening of their eigenlevels and this model is especially suitable for systems with very limited knowledge of lead-wire bonding structure. Transport properties of sodium nanowires are studied by this method and the odd-even oscillations of the conductance are reproduced.

Acknowledgments

The authors are grateful to F. Evers, M. Gelin and K. S. Thygesen for helpful discussion.

APPENDIX A: LORENTZIAN BROADENING OF ELECTRODES LEVELS

The density of states of the leads is related to imaginary part of Green's function by

$$\text{Im}g(E) = -\pi\mathbf{D}(E) \quad (\text{A1})$$

and real part of Green's function can then be obtained by Kramers-Koning relation

$$\text{Re}g(E) = \frac{1}{\pi}P \int_{-\infty}^{+\infty} \frac{\text{Im}g(\omega)}{\omega - E} d\omega. \quad (\text{A2})$$

Here P stands for the Cauchy principal value integral. For the widely used Gaussian broadening,²³ this procedure is numerically complicated (Romberg integration technique) and time-consuming. We use the Lorentzian broadening instead and we will show in this appendix that the broadening parameter in Lorentzian for the density of states is the same as the infinitesimal parameter in the non-interacting electrode Green's function. The Lorentzian broadening function is written as

$$D(E) = \frac{1}{\pi} \sum_i \frac{d_i \sigma}{(E - \epsilon_i)^2 + \sigma^2}, \quad (\text{A3})$$

where ϵ_i are the eigenlevels for the left or right electrode cluster. The Cauchy principal integral can be obtained analytically for the Lorentzian density of states and it yields the following Green's function matrix for the leads

$$g_{ij}(E) = \frac{\delta_{ij}}{(E - \epsilon_i)^2 + \sigma^2} (E - \epsilon_i - i\sigma) \quad (\text{A4})$$

or in matrix form

$$\begin{aligned} \mathbf{g}(E) &= \frac{\delta_{ij}}{(E - \mathbf{H})^2 + \sigma^2} (E - \mathbf{H} - i\sigma) \\ &= [(E + i\sigma)\mathbf{I} - \mathbf{H}]^{-1}. \end{aligned} \quad (\text{A5})$$

¹ A. Nitzan and M. A. Ratner, Science **300**, 1384 (2003).

² M. A. Reed, C. Zhou, C. J. Muller, T. P. Burgin, and J. M. Tour, Science **278**, 252 (1997).

³ X. D. Cui, A. Primak, X. Zarate, J. Tomfohr, O. F. Sankey, A. L. Moore, T. A. Moore, D. Gust, G. Harris, and S. M. Lindsay, Science **294**, 571 (2001).

⁴ B. Xu and N. J. Tao, Science **301**, 1221 (2003).

⁵ J. Taylor, H. Guo, and J. Wang, Phys. Rev. B **63**, 245407 (2001).

⁶ M. Brandbyge, J.-L. Mozos, P. Ordejón, J. Taylor, and K. Stokbro, Phys. Rev. B **65**, 165401 (2002).

⁷ Y. Xue, S. Datta, and M. Ratner, Chem. Phys. **281**, 151

- (2002).
- ⁸ F. Evers, F. Weigend, and M. Köntopp, Phys. Rev. B **69**, 235411 (2004).
 - ⁹ A. Calzolari, N. Mazari, I. Souza, and M. B. Nardelli, Phys. Rev. B **69**, 35108 (2004).
 - ¹⁰ K. S. Thygesen, and K. W. Jacobsen, Chem. Phys. in press (2005).
 - ¹¹ R.M. Martin, *Electronic structure. Basic theory and practical methods* Cambridge University Press, (2004).
 - ¹² K. S. Thygesen, L. B. Hansen, and K. W. Jacobsen, Phys. Rev. Lett. **94**, 26405 (2005).
 - ¹³ J. J. Mortensen and M. Parrinello, J. Phys.: Condens. Matter **13**, 5731 (2001).
 - ¹⁴ CPMD V3.9 Copyright IBM Corp 1990-2004, Copyright MPI fuer Festkoerperforschung Stuttgart 1997-2001.
 - ¹⁵ G. H. Wannier, Phys. Rev. **52**, 191 (1937).
 - ¹⁶ G. Berghold, C. J. Mundy, A. H. Romero, J. Hutter, and M. Parrinello, Phys. Rev. B **61**, 10040 (2000).
 - ¹⁷ N. Marzari and D. Vanderbilt, Phys. Rev. B **56**, 12847 (1997).
 - ¹⁸ I. Souza, N. Marzari, and D. Vanderbilt, Phys. Rev. B **65**, 35109 (2002).
 - ¹⁹ S. Datta, *Electronic Transport in Mesoscopic Systems* Cambridge University Press, (1997).
 - ²⁰ D. H. Lee and J. D. Joannopoulos, Phys. Rev. B **23**, 4988 (1981).
 - ²¹ D. H. Lee and J. D. Joannopoulos, Phys. Rev. B **23**, 4997 (1981).
 - ²² M. P. Lopez Sancho, J. M. Lopez Sancho, and J. Rubio, J. Phys. F: Met. Phys. **15**, 851 (1985).
 - ²³ T. Tada, M. Kondo, and K. Yoshizawa, J. Chem. Phys. **121**, 8050 (2004).
 - ²⁴ K. Lee, J. Callaway, and S. Dhar, Phys. Rev. B **30**, 1724 (1984).
 - ²⁵ J. Zhao, J. Yang, and J. G. Hou, Phys. Rev. B **67**, 85404 (2003).
 - ²⁶ J. M. Krans, J. M. van Ruitenbeek, V. V. Fisun, I. K. Yanson, and L. J. de Jongh, Nature **375**, 767 (1995).
 - ²⁷ J. M. Krans, J. M. van Ruitenbeek, and L. J. de Jongh, Phys. B **218**, 228 (1996).
 - ²⁸ A. I. Yanson, I. K. Yanson, and J. M. van Ruitenbeek, Nature **400**, 144 (1999).
 - ²⁹ N. D. Lang, Phys. Rev. Lett. **79**, 1357 (1997).
 - ³⁰ H. -S. Sim, H. -W. Lee, and K. J. Chang, Phys. Rev. Lett. **87**, 96803 (2001).
 - ³¹ S. Tsukamoto and K. Hirose, Phys. Rev. B **66**, 161402 (2002).
 - ³² Y. J. Lee, M. Brandbyge, M. J. Puska, J. Taylor, K. Stokbro, and R. M. Nieminen, Phys. Rev. B **69**, 125409 (2004).
 - ³³ P. A. Khomyakov and G. Brocks, Phys. Rev. B **70**, 195402 (2004).
 - ³⁴ X. Gonze, R. Stumpf, and M. Scheffler, Phys. Rev. B **44**, 8503 (1991).
 - ³⁵ W. T. Pollard and R. A. Friesner, J. Chem. Phys. **99**, 6742 (1993).
 - ³⁶ A. Alavi, J. Kohanoff, M. Parrinello, and D. Frenkel, Phys. Rev. Lett. **73**, 2599 (1994).
 - ³⁷ M. Brandbyge, M. R. Sorensen, and K. W. Jacobsen, Phys. Rev. B **56**, 14956 (1997).
 - ³⁸ We have also test the 10-atom cluster model, which is obtained by adding another layer to the electrode from the Na (001) surface. With smaller broadening parameters, the bigger model gives similar results as the 5-atom cluster model discussed in the text.
 - ³⁹ S. Datta and W. Tian, Phys. Rev. B **55**, R1914 (1997).